Chapter 16
Development of Bioactive Organic–Inorganic Hybrids Through Sol–Gel Processing

Toshiki Miyazaki, Masanobu Kamitakahara, and Chikara Ohtsuki

Abstract Bioactive ceramics have attractive features for bone repair because they spontaneously bond to a living bone when implanted in bony defects. However their clinical application is limited to repairs requiring only low loads of material due to their insufficient mechanical performance such as higher brittleness and lower flexibility than those of natural bones. It has been reported that the essential condition for artificial materials to show bioactivity is the formation of bone-like apatite on their surfaces through chemical reactions with body fluids. Fundamental studies concerning apatite formation on bioactive glasses and glass-ceramics have reported that the formation of surface apatite is triggered by both the release of calcium ions and by Si–OH groups formed on the surface of materials. These findings led the authors of the present chapter to the idea that new bioactive materials with mechanical properties similar to those of natural bones can be designed by organic modification of calcium silicate. After a brief critical review of the state-of-the-art on artificial bones, the authors report on their work, emphasizing how bioactive organic–inorganic hybrids have been designed and developed from various organic polymers by addition of Si–OH groups and calcium ions. Similar chemical modification is also effective for providing conventional polymethylmethacrylate (PMMA)-based bone cement with bioactivity. The added-value of bioactive organic–inorganic hybrids is experimentally demonstrated while future prospects show the promises of such new bionanocomposites.

T. Miyazaki (✉)
Graduate School of Life Science and Systems Engineering, Kyushu Institute of Technology,
2-4 Hibikino, Wakamatsu-ku, Kitakyushu, 808-0196, Japan
e-mail: tmiya@life.kyutech.ac.jp

M. Kamitakahara
Graduate School of Materials Science, Nara Institute of Science and Technology,
8916-5 Takayama-cho, Ikoma-shi, Nara 630-0192, Japan

C. Ohtsuki
Department of Crystalline Materials Science, Graduate School of Engineering,
Nagoya University, Furo-cho, Chikusa-ku, Nagoya 464-8603, Japan

L. Merhari (ed.), *Hybrid Nanocomposites for Nanotechnology*,
DOI: 10.1007/978-0-387-30428-1_16,

16.1 Introduction

Our body tissues and organs lose their functions due to diseases, accidents and aging. When the level of damage is not too severe, the tissues and functions can be spontaneously repaired by the self-reconstructing ability of the body through normal nutritious supply and recuperation. Reconstruction can be assisted by artificial means such as medicine, radial rays, and thermal treatment. However, when the damage to tissue is too large to benefit from full self-reconstruction, the lost tissue and function may induce further problems to peripheral tissues. In such a case, the damaged tissues are reconstructed with alternative materials. The most popular technique is called "autograft" and consists of transferring healthy tissue from another part of the body of the same patient. Autografting has the intrinsic problem of inducing damages to healthy tissues of the patient, because the bone graft is extracted from the patient himself. Another candidate technique is called "allograft" and consists of transferring tissues from other persons. The allograft faces problems of infection due to certain disease-causing substances when it is implanted into the patient. In addition, lack of donors is also a significant problem.

We therefore expect that artificial materials could be used to substitute or to support function of organs. Materials designed for such purposes are called biomaterials. Biomaterials are defined as materials intended to interface with biological systems in order to evaluate, treat, augment or replace any tissue, organ or function of the body. Several artificial materials including ceramics and metals have been used for repairing bony defects. However the problem is that materials implanted in bony defects get encapsulated by fibrous tissues to be isolated from the surrounding bone [1]. This is a normal reaction for protecting our living body from foreign substances. This type of biological response is called bioinertness.

16.2 Bioactive Ceramics

In the early 1970s, Hench et al. developed a novel glass, so-called Bioglass®, in the Na_2O–CaO–SiO_2–P_2O_5 system [2–4]. It has quite attractive characteristics for making direct bone-bonding in the body. This type of bone-bonding ability is called bioactivity. The typical composition (wt%) of this glass is Na_2O (24.5%), CaO (24.5%), SiO_2 (45%), P_2O_5 (6%). With such a composition, the glass displays the highest rate of bone-bonding among Na_2O–CaO–SiO_2–P_2O_5 systems. Bioglass® has such high biological affinity that it bonds not only to hard tissues but also to soft tissues. The high biological affinity of Bioglass® expands its clinical application to artificial middle ear, and fillers for alveolar ridge reconstruction. However, the mechanical strength of Bioglass® is as low as that of conventional glasses; therefore its clinical application is restricted to reconstructions where a large material loading is not required. Development of bioactive glass-ceramics has been undertaken in order to improve the mechanical properties of bioactive glasses. Kokubo et al. synthesized a bioactive glass-ceramic A-W, that has oxyfluorapatite ($Ca_{10}(PO_4)_6(O,F_2)$) and β-wollastonite crystals in the MgO–CaO–SiO_2 glassy matrix. This synthesis was based on heat-

treatment of a glass having the following composition in weight%: MgO (4.6%), CaO (44.7%), SiO_2 (34.0%), P_2O_5 (16.2%), CaF_2 (0.5%) [5, 6]. This glass-ceramic contains β–wollastonite ($CaO{\cdot}SiO_2$) which consists of silicate chains of SiO_4 in the tetrahedral structure, to increase its mechanical strength, as well as oxyfluorapatite. In other words, glass-ceramic A-W is a kind of ceramic–ceramic hybrid that contains 38 wt. % of oxyfluorapatite and 34 wt. % of β-wollastonite grains having a size of approximately 50–100 nm. Glass-ceramic A-W shows a bending strength of approximately 200 MPa in air, which is larger than that of the human cortical bone.

When a rectangular specimen of glass-ceramic A-W is implanted in a rabbit tibia, it bonds to the living bone within 4 weeks. It bonds so tightly that, after applying a load perpendicular to the interface a fracture occurred not within the glass-ceramics but within the bony tissues. Thanks to its excellent bioactivity and mechanical properties, the glass-ceramic A-W was clinically used as artificial iliac crest, vertebrae, and bone fillers from 1991 to 2000. Clinical applications involved this material in more than 45,000 cases until 2000.

Hydroxyapatite ($Ca_{10}(PO_4)_6(OH)_2$) is known as the main inorganic component of natural bones which comprise 70 wt % of bone matrix. Synthetic hydroxyapatite prepared by the sintering process also exhibits bioactivity [7]. It was commercialized in the late 1980s as bone substitute in the form of dense body, porous body and granules.

The sol–gel process is also suitable for synthesis of hydroxyapatite ceramics [8, 9]. Calcium alkoxide such as $Ca(OC_2H_5)_2$ and phosphorus alkoxide such as $P(OC_2H_5)_3$ and $PO(OC_2H_5)_3$ are often used as precursors. In this technique, the hydroxyapatite thin-films can be easily coated on various ceramics and metals [10].

Apatite cements are also developed to be applied as injectable bone substitutes. In these cements, a calcium phosphate paste is prepared by mixing powder of calcium phosphates in an aqueous liquid. The paste can be formed into desirable shapes for several minutes. It precipitates low-crystalline hydroxyapatite after setting and fills bone defects.

Brown and Chow developed apatite cement from tetracalcium phosphate (TTCP, $Ca_4(PO_4)_2O$) and anhydrous calcium hydrogen phosphate (DCPA, $CaHPO_4$) [11]. The setting reaction of the cement is as follows:

$$2Ca_4(PO_4)_2O + 2CaHPO_4 \rightarrow 10Ca^{2+} + 6PO_4^{3-} + 2OH^- \quad (16.1)$$

$$10Ca^{2+} + 6PO_4^{3-} + 2OH \rightarrow Ca_{10}(PO_4)_6(OH)_2 \quad (16.2)$$

Calcium and phosphate ions are released from TTCP and DCPD (dicalcium phosphate dihydrate) into the surrounding liquid after mixing the powder with the liquid. Solubility of TTCP and DCPA in water is higher than that of hydroxyapatite [1]. Therefore the surrounding liquid becomes supersaturated with respect to the apatite after dissolving of TTCP and DCPA. As a result, the cement sets through precipitation of the apatite, locking together the formed apatite crystals. The solubility of TTCP in water is higher than that of DCPA. In order to match the dissolution rates of TTCP and DCPD, the particle size of TTCP is adjusted to be ten times that of DCPA.

Monma et al. found that α-tricalcium phosphate (α-TCP) precipitates hydroxyapatite by hydrolysis as follows [12]:

$$10Ca_3(PO_4)_2 + 6H_2O \rightarrow 3Ca_{10}(PO_4)_6(OH)_2 + 2H_3PO_4$$

Apatite cement based on α-TCP has been also developed. However, the rate of hydrolysis of α-TCP is lower in comparison with the apatite precipitation of the cement based on TTCP and DCPD. In order to improve reactivity with the liquid, TTCP or an organic acid such as malic acid and succinic acid is added to the cement.

16.3 Bone-Bonding Mechanism of Bioactive Ceramics

According to earlier reports on the observation of the interface between the bioactive ceramics and the bone in vivo, these ceramics bond to the living bone through an apatite layer formed at the interface via a chemical reaction with the body fluid, as shown in Fig. 16.1 [13, 14]. Exceptionally, TCP ceramics exhibit bioactivity without formation of such an apatite layer [15]. This apatite layer is composed of carbonate hydroxyapatite with both a structure and a composition similar to those of natural bone. Therefore, it is expected that fibroblastic cells do not proliferate on the apatite layer, which results in a direct contact of the bone with the surface of the materials, without the fibrous tissue interfering. In the above case, a tight chemical bond may be formed between the surface apatite and the bone apatite in order to decrease

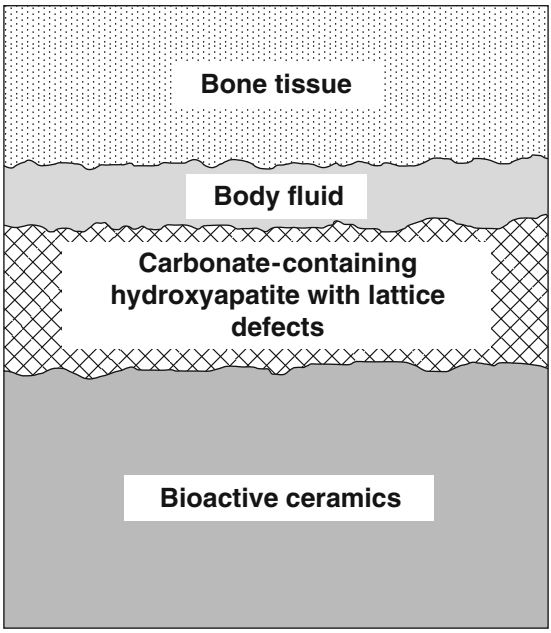

Fig. 16.1 Bone-bonding mechanism of bioactive ceramics

interface energy between them. The bone-bonding ability therefore depends on the rate of apatite formation when the materials are exposed to body fluids.

The apatite formation on bioactive ceramics and glass-ceramics can be well reproduced even in a simulated body fluid (SBF) that has concentrations of inorganic ions almost similar to those of the human blood plasma, as shown in Fig. 16.2 [16–19]. The apatite formation is caused by chemical reaction between the material surface and the surrounding fluid, because SBF does not contain any cell or protein. Materials which grow the apatite layer on their surface in SBF have the potential to bond to living bones. This SBF can be used for the evaluation of bioactivity of not only artificial materials in vitro, but also apatite coating on various materials under biomimetic conditions.

Ion concentrations of SBF are shown in Fig. 16.2. The pH of SBF is adjusted to pH 7.25 at 36.5°C. When the apatite-forming ability of the specimen is not very high, the pH of SBF is sometimes adjusted to 7.40. This fluid is a metastable solution containing calcium and phosphate ions and is already supersaturated with respect to the apatite. Therefore SBF is prepared as follows, using bottles and wares washed with HCl solution, neutral detergent, and ultrapure water. Firstly, 700 cm^3 of ion-exchanged distilled water is poured into a 1,000 cm^3 polyethylene bottle, and is stirred with a magnetic stirrer, and the reagent-grade chemicals are added into the water, one by one in the given order, after each reagent is completely dissolved. Temperature of the solution in the bottle is adjusted to 36.5°C with a water bath, and the pH of the solution to 7.25 by titrating 1 kmol/m^3 HCl solution. Once the pH is adjusted, the solution is transferred from the polyethylene bottle to a volumetric glass flask. Ultrapure water is added to adjust the total volume of the solution to one liter, and the flask is shaken. The solution is transferred from the flask to a polyethylene or polystyrene bottle, and stored in a refrigerator at 5–10°C. The fluid can be preserved for more than one month in a refrigerator. A solution with ion concentrations

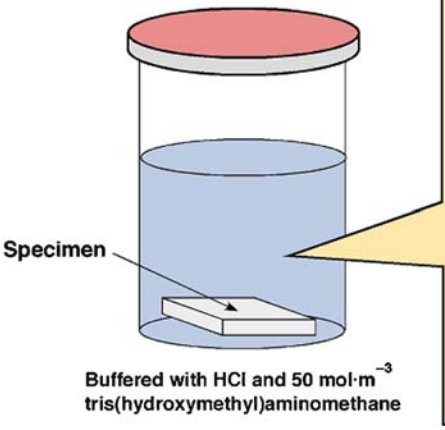

Ion	Concentration / mol·m^{-3}	
	SBF	Human blood plasma
Na^+	142.0	142.0
K^+	5.0	5.0
Mg^{2+}	1.5	1.5
Ca^{2+}	2.5	2.5
Cl^-	147.8	103.0
HCO_3^-	4.2	27.0
HPO_4^{2-}	1.0	1.0
SO_4^{2-}	0.5	0.5

Fig. 16.2 Ion concentrations of SBF in comparison with those of human blood plasma

1.5 times of SBF (1.5SBF) can be also prepared by following a modified protocol to accelerate the apatite formation in biomimetic apatite coating.

Although chemical reactions between materials and the body fluid in vitro are well reproduced in SBF, there is still a gap in the composition between SBF and the human extracellular fluid i.e. SBF contains larger amount of Cl^- ions and smaller amount of HCO_3^- ions. Therefore the apatite which was formed in SBF also contains a larger amount of Cl^- ions and a smaller amount of HCO_3^- than the natural bone. A novel simulated body fluid with inorganic ion concentrations exactly equal to those of the human extracellular fluid has been proposed by revising the protocol of preparation including the type and amount of chemical reagents [19, 20].

16.4 Basic Composition for Exhibiting Bioactivity

It was shown that bioactive materials can be designed by selecting a material with apatite-forming ability. The ability of apatite formation is dependent on the composition and structure of materials. For instance, the rate of apatite formation increases in the following order: sintered hydroxyapatite < glass-ceramic A-W < Bioglass® [21–23]. Sintered hydroxyapatite also forms a bone-like apatite phase when it is exposed to body fluids, through an ion-exchange reaction with those surrounding fluids [24, 25]. However the reaction rate is small. In contrast, the reaction rate is higher for glass-ceramic A-W which contains CaO, SiO_2-based glassy phase, as well as crystalline oxyfluorapatite and β-wollastonite. This glassy phase will contribute to rapid apatite deposition.

Which components constitute the basic composition of bioactive ceramics? Ohtsuki et al. fundamentally investigated the compositional dependence of apatite formation on the surface of glasses in the $CaO–SiO_2–P_2O_5$ system after soaking in SBF [26]. It was noted that surface apatite formation is restricted to areas composed of the (CaO, SiO_2) system, but not the (CaO, P_2O_5) system. Both the calcium ions released from (CaO, SiO_2)-based glasses and the phosphate ions released from (CaO, P_2O_5)-based glasses increased almost equally the degree of supersaturation of the surrounding fluid with respect to the apatite. In spite of that, the former glasses grow the surface apatite layer, but not the latter. This indicates that the surface of (CaO, SiO_2)-based glasses exclusively provides favorable sites for apatite nucleation.

The glasses form a silica hydrogel layer prior to forming the apatite layer and dissolve an appreciable amount of silicate ions. This means that highly hydrated silica, thus involving silanol (Si–OH) groups, is abundant on the surface of the glasses. It is speculated that the silanol groups effectively induce heterogeneous nucleation of the apatite. This is confirmed by the observation that a pure silica gel, prepared by a sol–gel method, forms bone-like apatite on its surface in a SBF at pH 7.40 [18, 27]. This suggests that a certain type of silanol groups is responsible for the apatite deposition on bioactive materials. The released Ca^{2+} ions will increase the degree of supersaturation of the surrounding fluid with respect to the apatite,

which is already supersaturated even before its exposure to the glass-ceramics. Once apatite nuclei are formed on the surface of the materials, they can grow spontaneously by consuming calcium and phosphate ions of the surrounding body fluid. Addition of a small amount of Al_2O_3 and TiO_2 significantly reduces the apatite formation in SBF [28, 29]. This is because the release of Ca^{2+} from the glasses into the surrounding fluid is suppressed, and the apatite-forming ability of hydrated silica containing Al_2O_3 and TiO_2 is thought to be lower than that of pure hydrated silica formed on $CaO–SiO_2$ glasses.

Li et al. prepared $CaO–SiO_2–P_2O_5$ glass powders by sol–gel process [30]. They showed that the apatite-forming ability of sol-gel-derived glasses was higher than that of melt-derived ones of the same composition. This is attributed to large pore volume and surface area of the sol-gel-derived glasses. They also showed that the sol–gel process can expand the SiO_2-content range across which the apatite formation in SBF can be observed, namely from 60 mol% in the melt-derived glasses to as large as 85 mol%.

The initial stage of the apatite formation on (CaO, SiO_2)-based bioactive glasses and on sintered hydroxyapatite has been precisely investigated by using techniques such as transmission electron microscopy (TEM), energy-dispersive X-ray (EDX) spectroscopy, and zeta potential measurements [24, 25, 31]. The results of the above research have revealed that the apatite formation progresses through the following mechanisms. Firstly, Ca^{2+} ions in SBF are selectively adsorbed onto negatively charged surfaces. Then phosphate ions are adsorbed on the Ca-rich surfaces to form a kind of amorphous calcium phosphate. Finally, the formed amorphous calcium phosphate is converted into low-crystalline apatite, since hydroxyapatite is a thermodynamically stable phase among calcium phosphates in neutral conditions. As a summary, selective adsorption of Ca^{2+} in SBF onto negatively charged surfaces of materials is a key issue for inducing apatite formation.

16.5 Design of Bioactive Organic–Inorganic Hybrids by the Sol–Gel Process

Based on the mechanism of apatite formation on bioactive glasses and glass-ceramics, hybrid materials with bone-bonding ability can be developed *via* organic modification of Si–OH and Ca^{2+} at the nanometer level. Molecular design of bioactive organic–inorganic hybrids is schematically illustrated in Fig. 16.3.

In order to develop such organic–inorganic hybrids, only limited heat treatment at lower temperature is allowed during synthesis, since organic polymers are prone to thermal decomposition. The sol–gel processing enables synthesis of various ceramics and oxide gels at lower temperature, and therefore is one of the attractive methods to prepare organic–inorganic hybrids.

Mackenzie et al. have already reported that organically-modified silicates can be synthesized from tetraethoxysilane (TEOS) with incorporation of poly(dimethylsiloxane) (PDMS). The synthesized organic–inorganic hybrid, called

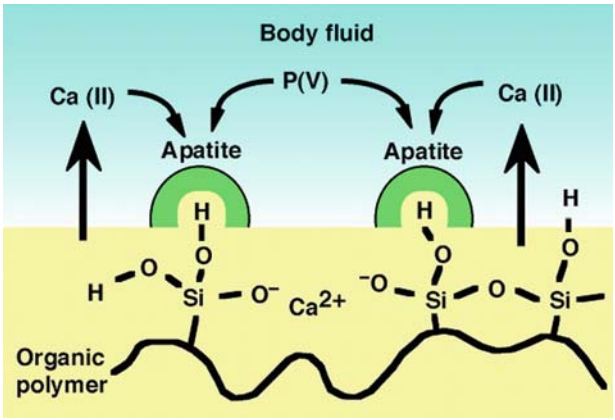

Fig. 16.3 Design of bioactive organic–inorganic composites

ORMOSIL, may combine the thermal stability of the silica block with the flexibility of the polymer chain [32].

Osaka et al. exploited the fact that ORMOSILS contain a lot of Si–OH groups and reported that incorporation of calcium nitrate in ORMOSILS during the sol–gel processing gave the hybrids the apatite-forming ability in SBF [33]. Si–OH groups and Ca^{2+} ions on ORMOSILS trigger nucleation of the apatite in SBF. This means that calcium salt-incorporated ORMOSILS show the bone-bonding property when implanted in the body. Chen et al. modified the protocol of synthesis and obtained TEOS–PDMS–$Ca(NO_3)_2$ hybrids with higher mechanical strength [34].

Synthesis of bioactive organic–inorganic hybrids has been also reported using vinyltrimethoxysilane (VS; $H_2C{=}CHSi(OCH_3)_3$) and methacyloxypropyl trimethoxysilane (MPS; $H_2C{=}CCH_3COO(CH_2)_3Si(OCH_3)_3$) as starting materials [35, 36]. Vinyl and methacryloyl groups in the starting organic substances were first radically polymerized to form organic polymers. The polymers were then incorporated with Ca^{2+} ions by mixing with calcium salts and subjected to hydrolysis with water to form Si–OH groups. The synthesized organic–inorganic hybrids formed an apatite layer on their surfaces in SBF.

16.6 Bioactive Organic–Inorganic Hybrids Synthesized from MPS and HEMA

We attempted the synthesis of bioactive organic–inorganic hybrids by incorporation of MPS ($CH_2{=}C(CH_3)COO(CH_2)_3Si(OCH_3)_3$) and calcium chloride into 2-hydroxyethylmethacrylate (HEMA, $CH_2{=}C(CH_3)COO(CH_2)_2OH$) [37]. HEMA has high hydrophilicity and biological affinity, and is used for medical applications such as contact lenses and coating agent on artificial blood vessels [38].

MPS and HEMA were dissolved in ethanol with a molar ratio of MPS:HEMA = 1:9, at a total concentration of 1 mol/dm^3. The solution of 100 cm^3 was heated at 75°C for 3 h with 0.001 mol benzoylperoxide (BPO) as initiator of the polymerization of HEMA and MPS. The obtained polymer solution was then mixed with 20 cm^3 of ethanol containing 0.01 mol calcium chloride ($CaCl_2$). In some of the solutions, addition of 1 cm^3 of either 1 mol/dm^3 HCl or 1 mol/dm^3 NH_3 aqueous solution catalyzed the hydrolysis. The resultant solutions were cast in polypropylene containers and dried at room temperature. After gelation, the gels were allowed to further dry under ambient condition at room temperature until weight loss of the sample became less than 2% in 24 h. Hybrids without and with addition of HCl and NH_3 were denoted as "NO", "HC" and "NH", respectively. Tensile mechanical properties of the hybrids were evaluated using a universal testing machine under ambient conditions according to Japanese Industrial Standard (JIS) K7113. Nine specimens were subjected to tensile test for NO, and seven specimens for HC and NH. Bioactivity of the obtained hybrids was evaluated by examining the apatite formation on their surfaces in SBF.

Figure 16.4 shows representative stress-strain curves for the MPS–HEMA hybrids. Their tensile strength increased in the following order: HC (0.15 ± 0.02 MPa) < NO (0.68 ± 0.04 MPa) < NH (2.10 ± 0.18MPa). Their Young's modulus also increased in the same order: HC (0.24 ± 0.02 MPa) < NO (2.65 ± 0.19 MPa) < NH (41.1 ± 1.8 MPa). The Young's modulus of the hybrids is quite similar to those of the human cancellous bone (50–500 MPa) and articular cartilage (1–10 MPa). Such hybrids are expected to bring a novel material for reconstruction of cancellous bones and articular cartilages.

SEM photographs of hybrids before and after soaking in SBF for 7 days are shown in Fig. 16.5. After soaking, spherical particles were formed on the surfaces of hybrids NO and NH, but not on the hybrid HC. TF–XRD patterns in Fig. 16.6

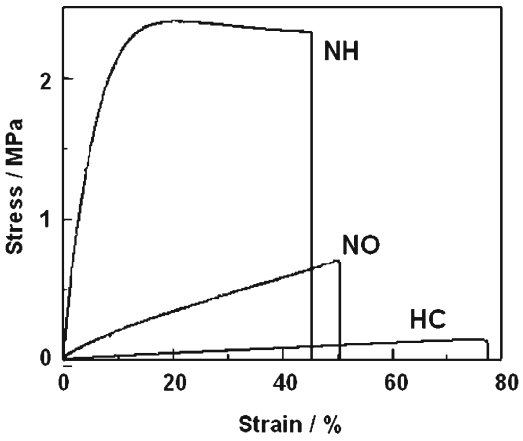

Fig. 16.4 Representative stress-strain curves of the MPS–HEMA hybrids prepared with different catalysts

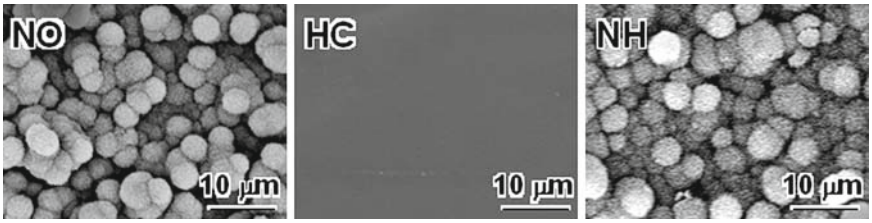

Fig. 16.5 SEM pictures of the MPS–HEMA hybrids prepared with different catalysts before and after soaking in SBF for 7 days

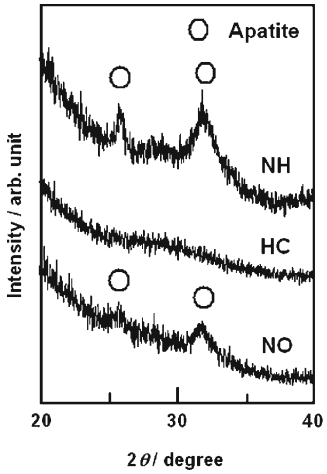

Fig. 16.6 TF–XRD patterns of surfaces of MPS–HEMA hybrids prepared with different catalysts before and after soaking in SBF for 7 days

show peaks assigned to poorly crystalline apatite at about 26° and 32° for hybrids NO and NH after the soaking, but not for the hybrid HC.

Our results indicate that hybrids NO and NH are expected to form apatite even in the body and bond to living bones. In contrast, hybrid HC does not show bioactivity, in spite of the existence of silanol groups and release of calcium ions. Release of HCl in hybrid HC decreases the degree of supersaturation of the surrounding fluid with respect to the apatite, and consequently suppresses apatite formation. There also remains the possibility that silanol groups did not have the appropriate structure after addition of HCl, because the structural effect of silica gel on the ability of apatite formation is also affected by the fabrication process of the silica gel [39, 40].

After polymerization of the MPS and HEMA solution, a copolymer consisting of MPS and HEMA is produced. The alkoxysilane groups in the copolymer are hydrolyzed by atmospheric water or catalysts to form silanol groups during aging and drying processes [41, 42]. The silanol groups then condense to form siloxane bonds (≡Si–O–Si≡), which allows cross-linking in the MPS–HEMA copolymer.

When HCl is added to the copolymer solution, linear siloxane chains are mainly formed by polycondensation of silanol groups [42]. In contrast, when NH_3 is added to the copolymer solution, 3-dimensional siloxane networks are predominantly formed. Therefore, hybrid NH has a harder structure caused by the high concentration of siloxane network, in comparison with hybrids NO and HC. The lower Young's modulus of hybrid HC may be attributed to a lower concentration of siloxane network in the hybrids structure.

Various natural and synthetic polymers are available for synthesis of hybrids. Recent research works have reported preparation of bioactive organic–inorganic hybrids from materials like chitosan and polycaprolactone *via* their modification with Si–OH and Ca^{2+} [43, 44].

16.7 Bioactive Starch-Based Hybrids

Starch is a natural organic polymer that is known as a constituent of various kinds of crop. Starch-based materials are getting a lot of attention as novel bone substitutes [45]. Miyazaki et al. attempted the preparation of bioactive organic–inorganic hybrids from starch by addition of glycidoxypropyltrimethoxysilane (GPS, $CH_2(O)CHCH_2O(CH_2)_3Si(OCH_3)_3$) and $CaCl_2$ [46].

In this procedure potato starch was dissolved in dimethylsulfoxide. $CaCl_2$, GPS, ultrapure water and divinylsulfone (DS) as cross-linking agent were then added to the solution. The prepared sol was subsequently poured into a Teflon dish and kept *in vacuum* at room temperature for 3 days to remove bubbles in the solution. It was then dried at 60°C for 21 days for further progress of the sol–gel reaction. Mass ratio of starch to the total of GPS and starch was fixed at 0.50, while the molar ratio of $CaCl_2$ to GPS was fixed at 0.05. Molar ratio of H_2O to GPS was fixed at 2.0. Mass ratio of divinylsulfone to starch was varied from 0 to 0.05. The specimen with (DS)/(DS + starch) = χ weight% was denoted as "DS x". The obtained gels were then soaked in SBF at pH 7.40 at 36.5°C for 7 days. Surface structural changes on the hybrids after soaking in SBF were examined by SEM and TF–XRD. Dumbbell-shaped specimens with the following dimensions were prepared: 115 mm in length, 25 ± 1 mm in width at the center and 6 ± 0.4 mm in width at the edges. Five specimens were subjected to tensile tests by using the Instron-type material testing machine, following the JIS 7127.

Figure 16.7 shows SEM pictures of the surfaces of the specimens after soaking in SBF for 7 days. Fine particles were observed on all the surfaces of the hybrids. The particles were identified as poorly crystalline apatite by TF–XRD. Figure 16.8 shows stress–strain curves of the representative specimens with various contents of divinylsulfone. Their tensile strength increased in the following order: DS0 (3.73 ± 0.66 MPa) < DS3 (9.68 ± 2.30 MPa) < DS5 (18.52 ± 1.27 MPa). Their Young's modulus also increased in the same order: DS0 (190 ± 20 MPa) < DS3 (292 ± 32 MPa) < DS5 (910 ± 36 MPa). The specimen with divinylsulfone 3 wt% to GPS showed mechanical properties analogous to those of human cancellous bones.

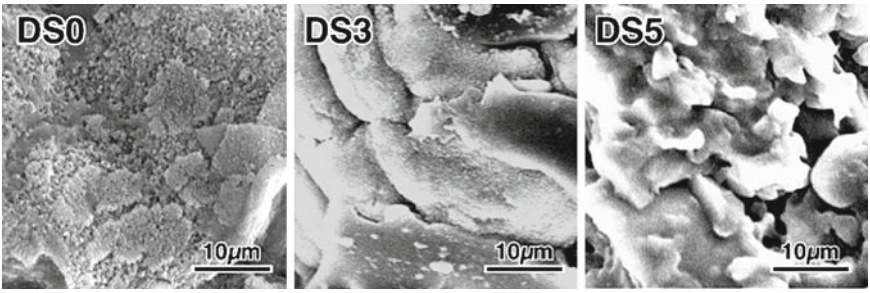

Fig. 16.7 SEM pictures of surfaces of GPS–starch hybrids with different divinylsulfone contents, after soaking in SBF for 7 days

Fig. 16.8 Representative stress-strain curves of GPS–starch hybrids with different divinylsulfone contents, before soaking in SBF

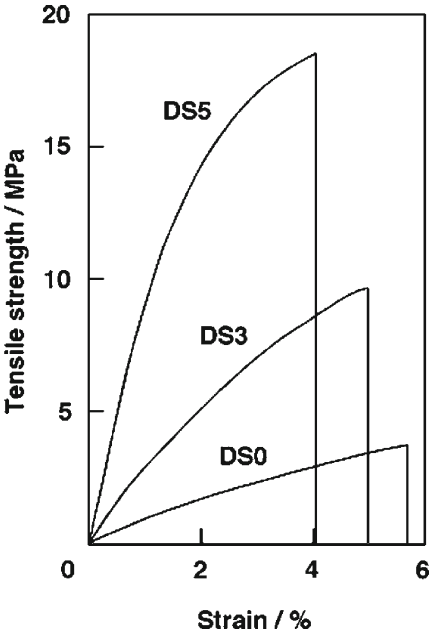

Organic–inorganic hybrids prepared from starch by addition of alkoxysilane and calcium salts were found to form apatite on their surfaces in SBF, irrespective of the divinylsulfone content. This means that addition of divinylsulfone as cross-linking agent does not generate an adverse effect on their bioactivity. Results of tensile tests show that the mechanical properties of the hybrids can be easily controlled by the content of cross-linking agent. The added divinylsulfone will bond to hydroxyl groups in starch to induce cross-linking, leading to improvement of the mechanical strength of the hybrid [47].

16.8 Bioactive Chitin-Based Hybrids

Chitin is a natural organic polymer, known as a constituent of club shell. Its chemical structure is shown in Fig. 16.9. Chitin has attractive features for implant materials, such as high hydrophilicity and low toxicity [48]. Miyazaki et al. attempted the preparation of bioactive organic–inorganic hybrids from chitin through modification with glycidoxypropyltrimethoxysilane (GPS, $CH_2(O)CHCH_2O(CH_2)_3Si(OCH_3)_3$) and calcium chloride ($CaCl_2$) [49].

Compositions of the prepared specimens are shown in Table 16.1. A powder of chitin was dissolved in *N*,*N*-dimethylacetamide (DMAc) solution containing lithium chloride (LiCl) at 6.6 weight%. Then GPS, divinylsulfone and $CaCl_2$ were added to the solution. The prepared sol solution was subsequently poured into a glass dish and dried in an air oven at 100°C for 24 h. The mass ratio of chitin to the total of GPS and chitin was fixed at 0.25, while the molar ratio of $CaCl_2$ to GPS ranged from 0 to 0.50. Ca-free gels were added with divinylsulfone to advance cross-linking. The bulk gels obtained were cut into rectangular specimens of 10 × 10 × 1 mm^3 section, and then soaked in 30 mL of SBF.

Homogeneous organic–inorganic hybrids can be successfully synthesized from chitin by modification with GPS and $CaCl_2$. Chitin is known to have high chemical durability due to tight intra- and intermolecular hydrogen bonds between the C=O groups and the N–H groups, and between the C=O groups and the OH groups [50]. Therefore chitin is quite difficult to dissolve in conventional aqueous and organic solvents. However, the LiCl/DMAc mixed solvent can easily dissolve chitin because Li^+ ions break the hydrogen bonds [51]. Bulk gels of organic–inorganic

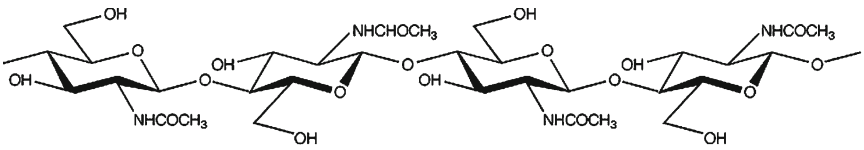

Fig. 16.9 Chemical structure of Chitin

Table 16.1 Compositions of GPS–Chitin hybrids

	Mass ratio		Molar ratio
Sample	Chitin/(Chitin+GPS)	DS/Chitin	$CaCl_2$/GPS
Ca0	0.25	0.05	0
Ca025	0.25	0	0.25
Ca05	0.25	0	0.50

GPS: Glycidoxyproyltrimethoxysilane
DS: Divinylsulfone

hybrid based on chitin can be synthesized using such a mixed solvent. Figure 16.10 shows SEM pictures of the surfaces of the specimens after soaking in SBF for 7 days. Deposition of fine particles was observed on the surfaces of all specimens after soaking. Figure 16.11 shows TF–XRD patterns of the surfaces of specimens

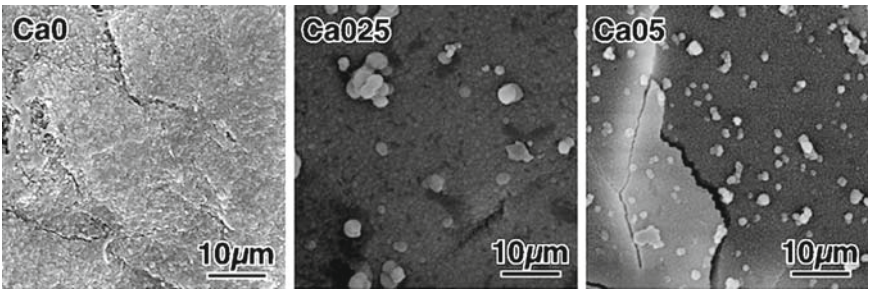

Fig. 16.10 SEM pictures of surfaces of GPS–Chitin hybrids with different calcium contents, after soaking in SBF for 7 days

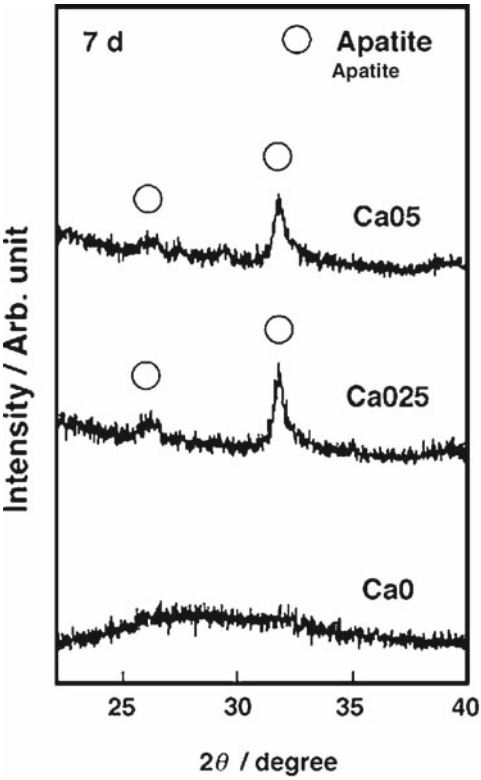

Fig. 16.11 TF-XRD patterns of surfaces of GPS–Chitin hybrids with different calcium contents, after soaking in SBF for 7 days

after soaking in SBF for 7 days. Broad peaks assigned to poorly crystalline apatite were observed at $2\theta = 26°$ and 32° in the XRD patterns of the specimens except for specimen Ca0 after soaking. Figure 16.12 shows EDX spectra of the surface of specimen Ca0 after soaking in SBF for 7 days. Peaks assigned to Ca and P were observed.

Even Ca-free hybrids grow a kind of calcium phosphate on their surface in SBF, although it is not identified as apatite. The apatite formation can be significantly enhanced by adding $CaCl_2$. This means that high bioactivity will be achieved on the chitin-based hybrids by addition of only a small amount of Ca^{2+}. It is reported that release of a large amount of Ca^{2+} in bioactive hybrids decreases the mechanical strength in body environment [52]. This type of chitin-based hybrid is attractive for flexible bone substitutes resistant to degradation in the body.

16.9 Bioactive Bone Cements Prepared by Organic Modification of Calcium Silicate

We applied organic modification of Si–OH and Ca^{2+} for the development of bioactive materials that can be injected into bony defects. Generally, bone cement consisting of poly(methyl methacrylate) (PMMA) powder and methyl methacrylate (MMA) liquid, in which they are mixed and polymerized, is clinically used for fixation of implants such as artificial hip joints [53]. Significant problems of the PMMA bone cement include loosening at the interface between the bone and the cement because

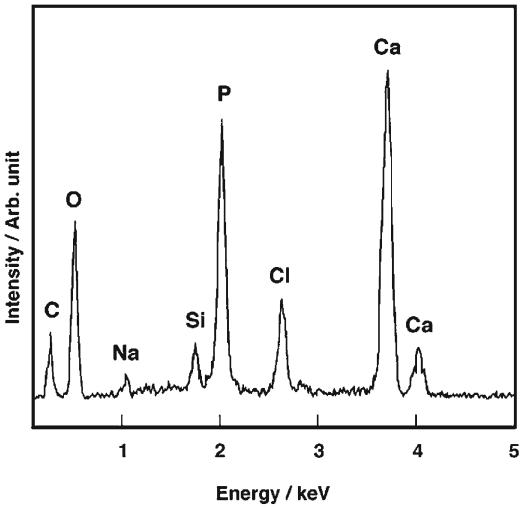

Fig. 16.12 EDX spectra of surface of sample Ca0 after soaking in SBF for 7 days

of a lack of bioactivity. Several studies have been conducted to develop bioactive cements through a method based on mixing powders of bioactive ceramics with the PMMA cement [54, 55]. In such a method, large amounts of ceramic powder should be incorporated into the cement to induce bioactivity, since the bioactive ceramic powder is almost covered with the PMMA matrix and thus hardly exposed to body fluids. Novel strategies for obtaining bioactive PMMA bone cements need to be therefore developed on the basis of a fundamental study on bonding mechanisms of artificial materials to living bones. We therefore attempted the preparation of bioactive PMMA bone cements by incorporating calcium silicate gels resulting from MPS and various calcium salts [56–58].

We used a PMMA powder having a molecular weight of about 100,000 and an average particle size about 14 μm. The PMMA powder was mixed with a calcium salt selected from $CaCl_2$, calcium acetate ($Ca(CH_3COO)_2$), calcium hydroxide ($Ca(OH)_2$), calcium lactate ($Ca(CH_3CHOHCOO)_2$) and calcium benzoate ($Ca(C_6H_5COO)_2$) at 20 wt% of the powder. BPO was then added to the powder as a polymerization initiator. MMA liquid was mixed with MPS at 20 wt% of the liquid. *N*,*N*-dimethyl-p-toluidine (NDT) was then added to the liquid as a polymerization accelerator. The composition of the cements is shown in Table 16.2. The cement denoted as "Reference" has a composition similar to that of the commercially available bone cement CMW®-1 (CMW Depuy), containing neither MPS nor calcium salt. The powder was mixed with the liquid at a powder to liquid ratio of 1:0.5 at 23 ± 2°C. The paste was shaped into a rectangular specimen with a size of $10 \times 15 \times 1$ mm^3. At half the setting time of the specimens, they were soaked in 35 cm^{-3} of SBF at pH 7.25 for 7 days to examine their apatite-forming ability. Compressive strengths of the cements with and without exposure to SBF were measured with a universal material testing machine.

Figure 16.13 shows SEM pictures of surfaces of cements modified with MPS and various kinds of calcium salts after soaking in SBF for 7 days. Assemblies of fine particles were observed on cements modified with $CaCl_2$, $Ca(CH_3COO)_2$ and $Ca(OH)_2$ after soaking. The formed particles were identified as poorly crystalline apatite by TF–XRD as shown in Fig. 16.14. Figure 16.15 reveals the compressive strengths of cements modified with MPS and various calcium salts before and after soaking in SBF for 7 days. The compressive strengths of modified cements decreased after exposure to SBF, except for cement modified with $Ca(OH)_2$. Of the cements examined in this study, those modified with $Ca(CH_3COO)_2$, $Ca(OH)_2$ or $Ca(CH_3CHOHCOO)_2$ showed a compressive strength close to the lower limit required by ISO5833.

Table 16.2 Compositions of cements

	Powder (Mass ratio)			Liquid (mass ratio)		
Sample	PMMA	Calcium Salt	BPO	MMA	MPS	NDT
Reference	0.971	0.000	0.029	0.992	0.000	0.008
Modified cement	0.776	0.194	0.029	0.794	0.198	0.008

MPS: Methacryloxypropyltrimethoxysilane
BPO: Benzoyl peroxide
NDT: N,N-dimethyl-p-toluidine

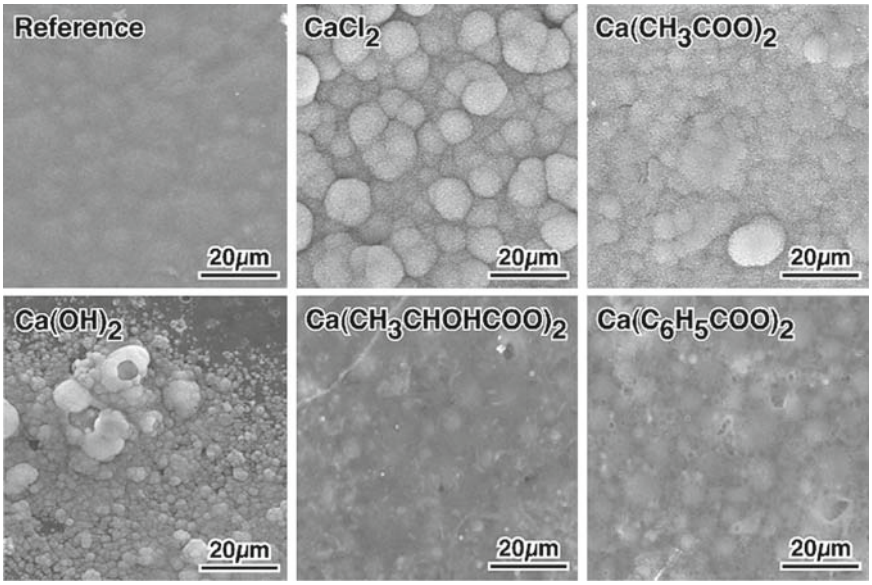

Fig. 16.13 SEM pictures of surfaces of cements modified with MPS and various kinds of calcium salts after soaking in SBF for 7 days

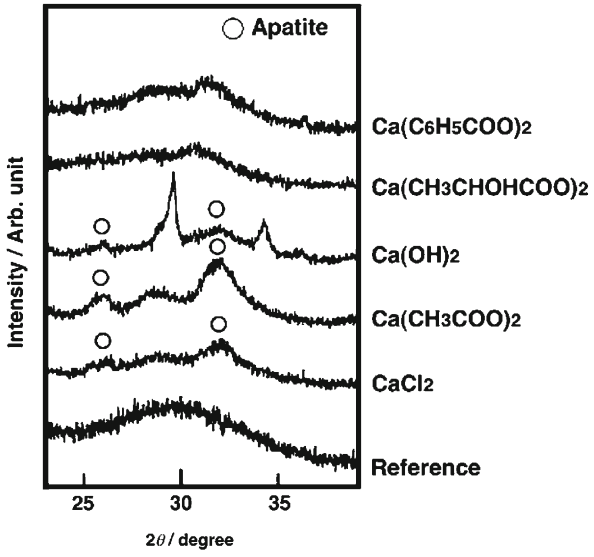

Fig. 16.14 TF-XRD patterns of surfaces of cements modified with MPS and various kinds of calcium salts after soaking in SBF for 7 days

Modification of PMMA cements by incorporation of MPS and appropriate types of calcium salts allows these cements to grow apatite when implanted in a patient body. Incorporated alkoxysilane and calcium salts form calcium silicate gels during setting and/or after exposure to SBF through sol–gel reaction. The formed calcium

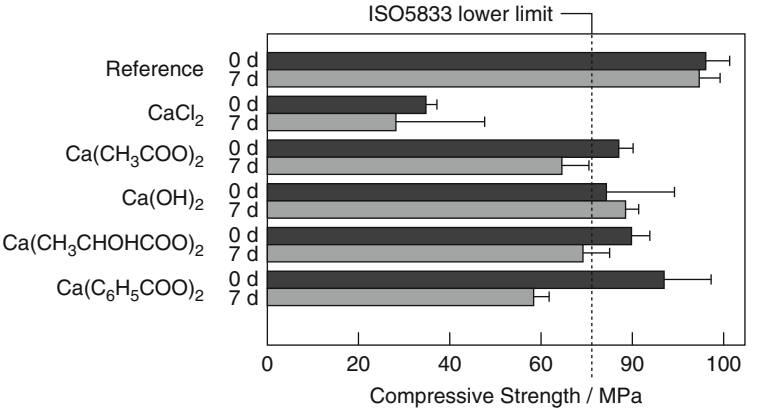

Fig. 16.15 Compressive strength of cements modified with MPS and various calcium salts before and after soaking in SBF for 7 days

silicate gels induce apatite nucleation in SBF. The solubility of the calcium salt in water decreases in the following order: $CaCl_2 > Ca(CH_3COO)_2 > Ca(CH_3CHOHCOO)_2 > Ca(C_6H_5COO)_2 > Ca(OH)_2$. Cements modified with highly water-soluble calcium salts have tendency to grow apatite in SBF. It is worth noting that cement modified with $Ca(OH)_2$ still formed apatite in SBF, despite the fact that the solubility of $Ca(OH)_2$ is the lowest compared to the calcium salts used in this study. The pH of the surrounding solution remarkably increased after soaking of cement modified with $Ca(OH)_2$ in SBF. The increase in pH accelerates the apatite nucleation, since OH^- is a component of the apatite. These observations indicate that increase in pH as well as release of Ca^{2+} govern the apatite formation on modified cements. All cements but that modified with $Ca(OH)_2$ showed a decrease in their compressive strength after soaking in SBF. This is attributed to release of Ca^{2+} ions from the cement into the solution. When Ca^{2+} ions are rapidly released, pores are formed inside the cement, leading to a decrease in compressive strength. An appropriate rate of release of Ca^{2+} is desirable to keep a high mechanical strength of the cement.

16.10 Bioactive Organic–Inorganic Hybrids Based on Various Metal Hydroxides

What kind of surface structure is effective for inducing bioactivity? In order to clarify this point, apatite deposition on various materials such as oxide gels prepared by sol–gel process, self-assembled monolayers (SAMs), and chemically-treated metal substrates was investigated in SBF. As a result, it appeared that not only Si–OH groups but also various functional groups such as Ti–OH [27, 59, 60], Zr–OH [61, 62], Ta–OH [63, 64], Nb–OH [65], Mo–OH [66], COOH [67–69],

PO_4H_2 [67] and SO_3H [70–72] are effective at triggering heterogeneous nucleation of the apatite. These findings led us to the idea that various bioactive organic–inorganic hybrids can be designed by organic modification of inorganic substances that provide the functional groups described above.

Uchida et al. reported that titania (TiO_2) having the anatase structure exhibits a higher ability for apatite formation in SBF than titania having either a rutile or an amorphous structure [60]. On the basis of these findings, Kamitakahara et al. synthesized bioactive anatase-poly(tetramethylene oxide) (PTMO) hybrids [73]. Anatase crystals with a size of about 10 nm precipitate after hot-water treatment of the organic–inorganic hybrids obtained from PTMO and titanium tetraisopropoxide ($Ti(OCH(CH_3)_2)_4$). The synthesized hybrids form the apatite in SBF within 3 days. It is worth noting that this type of hybrids grows the apatite, even if it does not contain Ca^{2+}. This means that Ca-free bioactive organic–inorganic hybrids can be designed by appropriately controlling the chemical state of the metal hydroxides. According to a similar molecular design, bioactive tantalum oxide (Ta_2O_5)–PTMO hybrids can be obtained [74]. Such Ca-free bioactive hybrids are expected to maintain their strength even in the patient body, in contrast to Ca-containing hybrids where release of Ca^{2+} is reported to decrease their strength in body fluids [52].

Miyazaki et al. prepared organic–inorganic hybrids based on poly(vinyl alcohol) (PVA) by modification with molybdenum hydroxide as well as hydrated silica, and compared their apatite-forming ability [75]. PVA is an organic polymer that has been studied extensively because of its high hydrophilicity, film-forming ability and processability [76, 77]. Further, in the medical field PVA is attractive for making artificial cartilages [78–80]. PVA with a molecular weight of 86,000 was dissolved in a mixed solvent of ultra-pure water and ethanol to form a 5 wt% solution at 80°C. Then followed the addition of tetraethoxysilane (TEOS, $Si(OC_2H_5)_4$) or bis(acetylacetonato) dioxomolybdenum(VI) (BADM, $MoO_2(CH_3COCHCOCH_3)_2$) under vigorous stirring, before $Ca(NO_3)_2$ was finally added to the solution. Compositions of the prepared hybrids are shown in Table 16.3.

Table 16.3 Compositions of PVA-based hybrids

		Mass ratio	Molar ratio
Sample	Alkoxide	Alkoxide/(PVA+Alkoxide)	$CaCl_2$/Alkoxide
Si60Ca007	TEOS	0.6	0.07
Si60Ca010	TEOS	0.6	0.10
Si60Ca015	TEOS	0.6	0.15
Mo40Ca10	BADM	0.4	1.0
Mo40Ca15	BADM	0.4	1.5
Mo40Ca20	BADM	0.4	2.0

TEOS: Tetraethoxysilane ($Si(OC_2H_5)_4$)
BADM: Bis(acetylacetonato) dioxomolybdenum (VI) ($MoO_2(CH_3COCHCOCH_3)_2$)

For all compositions, crack-free, homogeneous and transparent monolithic films were obtained. Figure 16.16 shows SEM pictures of the surfaces of PVA/silica and PVA/molybdenum oxide hybrids soaked in SBF. Numerous particles were observed on surfaces of all PVA/silica hybrids after soaking. In the case of PVA/molybdenum oxide hybrids, particles were observed on the surface of hybrids after the soaking when Ca/Mo molar ratio was 1.5 or more. Figure 16.17 shows TF–XRD patterns of surfaces of PVA/silica and PVA/molybdenum oxide hybrids soaked in SBF. Broad peaks assigned to low crystalline apatite were detected for all the examined PVA/silica hybrids. On the other hand, peaks assigned to the apatite were observed for PVA/molybdenum oxide hybrids with Ca/Mo molar ratio of 1.5 or more. In addition, peaks ascribed to calcium molybdate were detected for samples described above after the soaking.

The results show that bioactive organic–inorganic hybrids can be obtained through the sol–gel process from PVA by addition of silicon or molybdenum alkoxide, as well as calcium salt. Compared to PVA/Silica hybrids, addition of larger amount of calcium salt is necessary to induce the apatite formation on PVA/molybdenum oxide hybrids. Results of TF–XRD indicate that a kind of calcium molybdate as well as apatite is formed on the former after soaking in SBF. It is assumed that Ca^{2+} ions incorporated into the PVA/molybdenum oxide hybrids bind to not only phosphate ions but also molybdenum hydroxide to form water-insoluble calcium molybdate. These phenomena consequently suppress the release of Ca^{2+}, leading to lower ability of the apatite formation. It is also assumed that Mo–OH groups on surfaces of hybrids have lower apatite-forming ability than Si–OH counterparts.

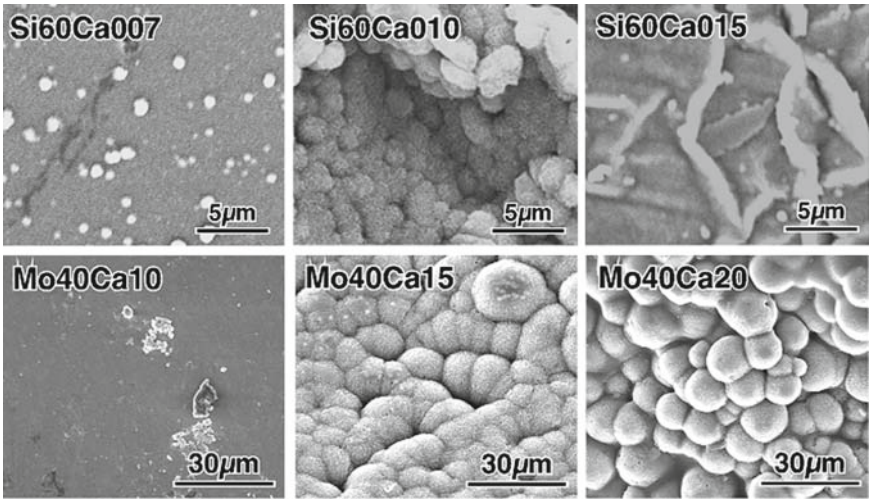

Fig. 16.16 SEM pictures of surfaces of PVA-based hybrids modified with silicon or molybdenum alkoxide, after soaking in SBF. Soaking period was 2 days and 3 days for PVA/silica and PVA/molybdenum oxide hybrids, respectively

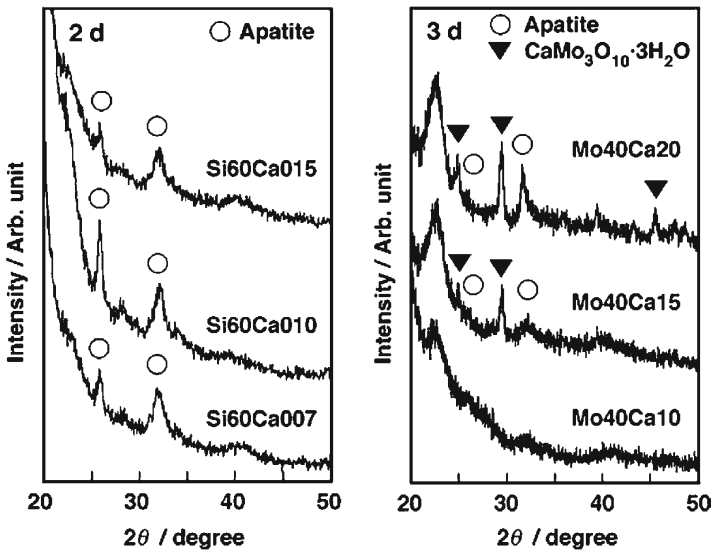

Fig. 16.17 TF-XRD patterns of surfaces of PVA-based hybrids modified with silicon or molybdenum alkoxide, after soaking in SBF. Soaking period was 2 days and 3 days for PVA/silica and PVA/molybdenum oxide hybrids, respectively

16.11 Conclusion

After carefully selecting various kinds of oxide gels that induce apatite deposition when in body fluids, bone-bonding bioactive nanohybrids can be designed by chemical modification of these gels with flexible organic polymers. Sol–gel process is a promising technique for obtaining such nanohybrids, and the described strategy of material design is expected to produce novel high-added-value biomaterials.

Acknowledgments This study was supported by a Grant-in-Aid for Encouragement of Young Scientists ((B)16700365) of the Japanese Society for the Promotion of Science.

References

1. Hench LL, Wilson J (1993) An Introduction to Bioceramics. World Scientific, Singapore
2. Hench LL, Splinger RJ, Allen WC, Greenlee TK (1972) Bonding mechanisms at the interface of ceramic prosthetic materials. J Biomed Mater Res Symp 2:117–141
3. Hench LL (1991) Bioceramics: from concept to clinic. J Am Ceram Soc 74:1487–1510
4. Hench LL (1998) Bioceramics. J Am Ceram Soc 81:1705–1728
5. Kokubo T, Shigematsu M, Nagashima Y, Tashiro M, Nakamura T, Yamamuro T, Higashi S (1982) Apatite- and Wollastonite-containing glass-ceramics for prosthetic application. Bull Inst Chem Res Kyoto Univ 60:260–268

6. Kokubo T, Kim HM, Kawashita M (2003) Novel bioactive materials with different mechanical properties. Biomaterials 24:2161–2175
7. Jarcho M (1976) Hydroxyapatite synthesis and characterization in dense polycrystalline forms. J Mater Sci 11:2027–2035
8. Deptula A, Lada W, Olczak T, Borello A, Alvani C, Dibartolomeo A (1992) Preparation of spherical powders of hydroxyapatite by sol-gel process. J Non-Cryst Solids 147:537–541
9. Jillavenkatesa A, Condrate RASr (1998) Sol-gel processing of hydroxyapatite. J Mater Sci 33:4111–4119
10. Chai CS, Ben-Nissan B (1999) Bioactive nanocrystalline sol–gel hydroxyapatite coatings. J Mater Sci Mater Med 10:465–469
11. Chow LC (1991) Development of self-setting calcium phosphate cements. J Ceram Soc Jpn 99:954–964
12. Monma H (1987) Tricalcium Phosphate Ceramics Complexed with Hydroxyapatite. Yogyo-Kyokai-Shi 95:814–818
13. Ohtsuki C, Kushitani H, Kokubo T, Kotani S, Yamamuro T (1991) Apatite formation on the surface of ceravital-type glass-ceramic in the body. J Biomed Mater Res 25:1363–1370
14. Neo M, Kotani S, Nakamura T, Yamamuro T, Ohtsuki C, Kokubo T, Bando Y (1992) A comparative study of ultrastructures of the interfaces between four kinds of surface-active ceramic and bone. J Biomed Mater Res 26:1419–1432
15. Ohtsuki C, Kokubo T, Neo M, Kotani S, Yamamuro T, Nakamura T, Bando Y (1991) Bone-bonding mechanism of sintered β-3CaO·P_2O_5. Phosphorus Res Bull 1:191–196
16. Kokubo T, Kushitani H, Sakka S, Kitsugi T, Yamamuro T (1990) Solutions able to reproduce in vivo surface-structure changes in bioactive glass-ceramic A-W. J Biomed Mater Res 24:721–734
17. Ohtsuki C, Aoki Y, Kokubo T, Bando Y, Neo M, Nakamura T (1995) Transmission electron microscopic observation of glass-ceramic A-W and apatite layer formed on its surface in a simulated body fluid. J Ceram Soc Jpn 103:449–454
18. Cho SB, Nakanishi K, Kokubo T, Soga N, Ohtsuki C, Nakamura T, Kitsugi T, Yamamuro T (1995) Dependence of apatite formation on silica gel on its structure: effect of heat treatment. J Am Ceram Soc 78:1769–1774
19. Kokubo T, Takadama H (2006) How useful is SBF in predicting in vivo bone bioactivity? Biomaterials 27:2907–2915
20. Oyane A, Kim HM, Furuya T, Kokubo T, Miyazaki T, Nakamura T (2003) Preparation and assessment of revised simulated body fluid. J Biomed Mater Res 65A:188–195.
21. Oonishi H, Kushitani S, Yasukawa E, Iwaki H, Hench LL, Wilson J, Tsuji E, Sugihara T (1997) Particulate bioglass compared with hydroxyapatite as a bone graft substitute. Clin Ortho Rel Res 334:316–325
22. Oonishi H, Murata N, Saito M, Wakitani S, Imoto K, Kim N, Matsuura M (1998) Comparison of bone growth behavior into spaces of hydroxyapatite and AW glass ceramic particles. In: LeGeros RZ, LeGeros JP (eds) Bioceramics Vol. 11. World Scientific, Singapore, pp. 411–414
23. Oonishi H, Hench LL, Wilson J, Tsuji E, Kin S, Yamamoto T, Mizokawa S (2000) Quantitative comparison of bone growth behavior in granules of Bioglass®, A-W glass-ceramic, and hydroxyapatite. J Biomed Mater Res 51:37–46
24. Kim HM, Himeno T, Kokubo T, Nakamura T (2005) Process and kinetics of bonelike apatite formation on sintered hydroxyapatite in a simulated body fluid. Biomaterials 26:4366–4373
25. Kim HM, Himeno T, Kawashita M, Kokubo T, Nakamura T (2004) The mechanism of biomineralization of bone-like apatite on synthetic hydroxyapatite: an in vitro assessment. J R Soc Interface 1:17–22.
26. Ohtsuki C, Kokubo T, Yamamuro T (1992) Mechanism of apatite formation on CaO-SiO_2-P_2O_5 glasses in a simulated body fluid. J Non-Cryst Solids 143:84–92
27. Li P, Ohtsuki C, Kokubo T, Nakanishi K, Soga N, de Groot K (1994) The role of hydrated silica, titania, and alumina in inducing apatite on implants. J Biomed Mater Res 28:7–15
28. Ohtsuki C, Kokubo T, Yamamuro T (1992) Compositional dependence of bioactivity of glasses in the system CaO-SiO_2-Al_2O_3: its in vitro evaluation. J Mater Sci Mater Med 3:119–125

29. Ohtsuki C, Osaka A, Kokubo T (1994) Effects of Al_2O_3 and TiO_2 on bioactivity of CaO-SiO_2 glasses. In Andersson OH, Yli-Urpo A (eds) Bioceramics Vol. 7. Butterworth-Heinemann, Oxford, pp. 73–78
30. Li R, Clark AE, Hench LL (1991) An investigation of bioactive glass powders by sol–gel processing. J Appl Biomater 2:231–239
31. Takadama H, Kim HM, Kokubo T, Nakamura T (2000) Mechanism of apatite formation induced by silanol groups-TEM observation. J Ceram Soc Jpn 108:118–121
32. Hu Y, Mackenzie JD (1992) Rubber-like elasticity of organically modified silicates. J Mater Sci 27:4415–4420
33. Tsuru K, Ohtsuki C, Osaka A, Iwamoto T, Mackenzie JD (1997) Bioactivity of sol–gel derived organically modified silicates, Part I: in vitro examination. J Mater Sci Mater Med 8:157–161
34. Chen Q, Miyaji F, Kokubo T, Nakamura T (1999) Apatite formation on PDMS-modified CaO-SiO_2-TiO_2 hybrids prepared by sol–gel process. Biomaterials 20:1127–1132
35. Osaka A, Ohtsuki C, Tsuru K (1995) Preparation of bioactive polymers modified with silanol groups. In: Wilson J, Hench LL, Greenspan D (eds), Bioceramics Vol. 8. Elsevier Science, Oxford, pp. 441–445
36. Yabuta T, Tsuru K, Hayakawa S, Ohtsuki C, Osaka A (2000) Synthesis of bioactive organic–inorganic hybrid with γ-methacryloxypropyl trimethoxysilane. J Sol-Gel Sci Tech 19:745–748
37. Miyazaki T, Ohtsuki C, Tanihara M (2003) Synthesis of bioactive organic–inorganic nanohybrid for bone repair through Sol–gel processing. J Nanosci Nanotech 3:511–515
38. Ratner BD, Hoffman AS, Schoen FJ, Lemons JE (2004) Biomaterials science 2nd edition, Elsevier Academic Press, Amsterdam
39. Cho SB, Nakanishi K, Kokubo T, Soga N, Ohtsuki C, Nakamura T (1996) Apatite formation on silica gel in simulated body fluid: its dependence on structures of silica gels prepared in different media. J Biomed Mater Res (Appl. Biomater.) 33:145–151
40. Cho SB, Miyaji F, Kokubo T, Nakanishi K, Soga N, Nakamura T (1998) Apatite formation on silica gel in simulated body fluid: effects of structural modification with solvent-exchange. J Mater Sci Mater Med 9:279–284
41. Plueddemann EP (1991) Silane Coupling Agents 2nd edition, Plenum, New York
42. Brinker CJ, Scherer GW (1990) Sol–Gel Science, Academic Press, San Diego
43. Yamada A, Tsuru K, Hayakawa S, Osaka A (2002) Chitosan-organosiloxane hybrids for biomedical applications. In: Abstract of the 3rd Asian international Symposium on Biomaterials and Drug Delivery Systems
44. Rhee SH (2004) Bone-like apatite-forming ability and mechanical properties of poly(ε-caprolactone)/silica hybrid as a function of poly(ε-caprolactone) content. Biomaterials 25:1167–1175
45. Mendes SC, Reis RL, Bovell YP, Cunha AM, van Blitterswijk CA, de Bruijn JD (2001) Biocompatibility testing of novel starch-based materials with potential application in orthopaedic surgery: a preliminary study. Biomaterials 22:2057–2064
46. Miyazaki T, Yasunaga S, Ishida E, Ashizuka M, Ohtsuki C (2005) Development of bioactive organic–inorganic hybrid based on starch. J Jpn Soc Powder and Powder Metall 52:360–363 (in Japanese)
47. Kabra BG, Gehrke SH, Spontak RJ (1998) Microporous, responsive hydroxypropyl cellulose gels. 1. Synthesis and microstructure. Macromolecules 31:2166–2173
48. Khor E. (2001) Chitin: Fulfilling a Biomaterials Promise, Elsevier, Amsterdam
49. Miyazaki T, Ohtsuki C, Tanihara M, Ashizuka M (2004) Apatite deposition on organic–inorganic hybrids prepared from chitin by modification with alkoxysilane and calcium salt. In: Barbosa MA, Monteiro FJ, Correia R, Leon B(eds), Bioceramics Vol. 16. Trans Tech Publications, Switzerland, pp. 545–548.
50. Khor E, Lim LY (2003) Implantable applications of chitin and chitosan. Biomaterials 24:2339–2349
51. Chen BQ, Sun K, Zhang KB (2004) Rheological properties of chitin/lithium chloride, N,N-dimethyl acetamide solutions. Carbohydr Polym 58:65–69

52. Kamitakahara M, Kawashita M, Miyata N, Kokubo T, Nakamura T (2004) Degradation of bioactive polydimethylsiloxane-CaO-SiO_2-TiO_2 and poly(tetramethylene oxide)-CaO-TiO_2 hybrids in a simulated body fluid. J Am Ceram Soc 87:235–239
53. Kühn KD (2000) Bone Cement. Springer, Berlin
54. Harper EJ (1998) Bioactive bone cements. Proc Inst Mech Eng H 212:113–120
55. Shinzato S, Kobayashi M, Mousa WF, Kamimura M, Neo M, Kitamura Y, Kokubo T, Nakamura T (2000) Bioactive polymethyl methacrylate-based bone cement: comparison of glass beads, apatite- and wollastonite-containing glass-ceramic, and hydroxyapatite fillers on mechanical and biological properties. J Biomed Mater Res 51:258–272
56. Ohtsuki C, Miyazaki T, Kyomoto M, Tanihara M, Osaka A (2001) Development of bioactive PMMA-based cement by modification with alkoxysilane and calcium salt. J Mater Sci Mater Med 12:895–899
57. Miyazaki T, Ohtsuki C, Kyomoto M, Tanihara M, Mori A, Kuramoto K (2003) Bioactive PMMA bone cement prepared by modification with methacryloxypropyltrimethoxysilane and calcium chloride. J Biomed Mater Res 67A:1417–1423
58. Mori A, Ohtsuki C, Sugino A, Kuramoto K, Miyazaki T, Tanihara M, Osaka A (2003) Bioactive PMMA-based bone cement modified with methacyloxypropyltrimetoxysilane and calcium salts - effects of calcium salts on apatite-forming ability. J Ceram Soc Jpn 111:738–742
59. Kim HM, Miyaji F, Kokubo T, Nakamura T (1996) Preparation of bioactive Ti and its alloys via simple chemical surface treatment. J Biomed Mater Res 32:409–417
60. Uchida M, Kim HM, Kokubo T, Fujibayashi S, Nakamura T (2003) Structural dependence of apatite formation on titania gels in a simulated body fluid. J Biomed Mater Res A 64:164–170
61. Uchida M, Kim HM, Kokubo T, Miyaji F, Nakamura T (2001) Bonelike apatite formation induced on zirconia gel in a simulated body fluid and its modified solutions. J Am Ceram Soc 84:2041–2044
62. Uchida M, Kim HM, Miyaji F, Kokubo T, Nakamura T (2002) Apatite formation on zirconium metal treated with aqueous NaOH. Biomaterials 23:313–317
63. Miyazaki T, Kim HM, Miyaji F, Kokubo T, Kato H, Nakamura T (2000) Bioactive tantalum metal prepared by NaOH treatment. J Biomed Mater Res. 50:35–42
64. Miyazaki T, Kim HM, Kokubo T, Kato H, Nakamura T (2001) Induction and acceleration of bonelike apatite formation on tantalum oxide gel in simulated body fluid. J Sol–gel Sci Tech 21:83–88
65. Miyazaki T, Kim HM, Kokubo T, Ohtsuki C, Nakamura T (2001) Bonelike apatite formation induced on niobium oxide gels in simulated body fluid. J Ceram Soc Jpn 109:934–938
66. Wakabayashi G, Miyazaki T, Ishida E, Ashizuka M, Kokubo T, Ohtsuki C (2003) Development of bioactive molybdenum metal by alkali treatment. In Okazaki M, Ishikawa K, Yamashita K, Doi Y, Ban S (eds), Archives of BioCeramics Research Vol. 3. Saga Printings, pp. 288–292
67. Tanahashi M, Matsuda T (1997) Surface functional group dependence on apatite formation on self-assembled monolayers in a simulated body fluid. J Biomed Mater Res 34:305–315
68. Kawashita M, Nakao M, Minoda M, Kim HM, Beppu T, Miyamoto T, Kokubo T, Nakamura T (2003) Apatite-forming ability of carboxyl group-containing polymer gels in a simulated body fluid. Biomaterials 24:2477–2484
69. Miyazaki T, Ohtsuki C, Akioka Y, Tanihara M, Nakao J, Sakaguchi Y, Konagaya S (2003) Apatite deposition on polyamide films containing carboxyl group in a biomimetic solution. J Mater Sci Mater Med 14:569–574
70. Kawai T, Ohtsuki C, Kamitakahara M, Miyazaki T, Tanihara M, Sakaguchi Y, Konagaya S (2004) Coating of apatite layer on polyamide films containing sulfonic groups by biomimetic process. Biomaterials 25:4529–4534
71. Miyazaki T, Imamura M, Ishida E, Ashizuka M, Ohtsuki C, Tanihara M (2005) Apatite formation on organic–inorganic hybrid containing sulfonic group. In Li P, Zhang K, Colwell CWJr (eds), Bioceramics Vol. 17. Trans Tech Publications, Switzerland, pp. 725–728

72. Leonor IB, Kim HM, Balas F, Kawashita M, Reis RL, Kokubo T, Nakamura T (2005) Surface charge of bioactive polyethylene modified with -SO_3H groups and its apatite inducing capability in simulated body fluid. In Li P, Zhang K, Colwell CWJr (eds) Bioceramics Vol. 17. Trans Tech Publications, Switzerland, pp. 453–456
73. Kamitakahara M, Kawashita M, Miyata N, Kokubo T, Nakamura T (2003) Apatite-forming ability and mechanical properties of CaO-free poly(tetramethylene oxide) (PTMO)-TiO_2 hybrids treated with hot water. Biomaterials 24:1357–1363
74. Kamitakahara M, Kawashita M, Miyata N, Kim HM, Kokubo T, Ohtsuki C, Nakamura T (2004) Apatite-forming ability and mechanical properties of poly(tetramethylene oxide) (PTMO)-Ta_2O_5 hybrids. In Barbosa MA, Monteiro FJ, Correia R, Leon B (eds), Bioceramics Vol. 16. Trans Tech Publications, Switzerland, pp. 521–524.
75. You C, Miyazaki T, Ishida E, Ashizuka M, Ohtsuki C, Tanihara M (2005) Apatite deposition on organic–inorganic hybrids synthesized from poly(vinyl alcohol) and various metal oxides. In Li P, Zhang K, Colwell CWJr (eds), Bioceramics Vol. 17. Trans Tech Publications, Switzerland, pp. 469–472
76. Huang RYM, Rhim JW (1993) Modification of poly(vinyl alcohol) using maleic-acid and its application to the separation of acetic-acid water mixtures by the pervaporation technique. Polym Int 30:129–135
77. Gimenez V, Mantecon A, Cadiz V (1996) Modification of poly(vinyl alcohol) with acid chlorides and crosslinking with difunctional hardeners. J Polym Sci A Polym Chem 34:925–934
78. Oka M, Ushio K, Kumar P, Ikeuchi K, Hyon SH, Nakamura T, Fujita H (2000) Development of artificial articular cartilage. Proc Inst Mech Eng H J Eng Med 214:59–68
79. Kobayashi M, Oka M (2004) Characterization of a polyvinyl alcohol-hydrogel artificial articular cartilage prepared by injection molding. J Biomater Sci Polym Ed 15:741–751
80. Nakashima K, Sawae Y, Murakami T (2005) Study on wear reduction mechanisms of artificial cartilage by synergistic protein boundary film formation. JSME Int J Ser C 48:555–561